Prepared for submission to Nature

Supplementary Information
A 2D-CFT Factory: Critical Lattice Models from Competing Anyon Condensation in SymTO

Ling-Yan Hung[1][a,c] **Kaixin Ji**[b] **Ce Shen**[c] **Yidun Wan**[2][b,d,e] **Yu Zhao**[b]

[a] *Yau Mathematical Sciences Center, Tsinghua University, Beijing 100084, China*

[b] *State Key Laboratory of Surface Physics, Center for Astronomy and Astrophysics, Department of Physics, Center for Field Theory and Particle Physics, and Institute for Nanoelectronic devices and Quantum Computing, Fudan University, 2005 Songhu Road, Shanghai 200433, China*

[c] *Beijing Institute of Mathematical Sciences and Applications, Beijing 101408, China*

[d] *Shanghai Research Center for Quantum Sciences, 99 Xiupu Road, Shanghai 201315, China*

[e] *Hefei National Laboratory, Hefei 230088, China*

E-mail: lyhung@tsinghua.edu.cn, kxji21@m.fudan.edu.cn, scbebetterme@gmail.com, ydwan@fudan.edu.cn, yuzhao20@fudan.edu.cn

[1] Corresponding author

[2] Corresponding author

1 The HGW String-Net Model

The HGW model [1–3] can be defined on a trivalent lattice, where a tail (purple lines in Fig. 3) is attached to a chosen edge of a plaquette, while the choice is topologically irrelevant . The lattice shape is irrelevant in the string-net model describing topological orders, but it plays an important role in conformal field theories. In this article, for convenience, we only define the HGW model on the truncated square lattice as shown in Figure 3, which facilitates the subsequent renormalization group procedure. The basic configuration is established by labeling each edge and tail with a simple object from the input unitary fusion category $\mathscr{F}$ of the HGW model, subject to the constraint on all vertices that $\delta_{ijk} = 1$ for the three incident edges or tails meeting at this vertex. The Hilbert space $\mathcal{H}$ of the model is spanned by all possible configurations of these labels on the edges and tails. Edges and tails are oriented, but the choice of orientation does not affect the physics.

In the HGW model, anyons reside on the plaquettes of the lattice, and their types are labeled by the simple objects of the Drinfeld center $\mathcal{Z}(\mathscr{F})$ of the input UFC $\mathscr{F}$. A key pro of the HGW construction is that it explicitly manifests the internal gauge degrees of freedom of non-Abelian anyons. Specifically, anyons are realized in the model by *dyons*—a pair consisting of an anyon type J and its internal gauge degree of freedom p, where p is the degree of freedom on the tail of the plaquette where the anyon resides. A given anyon type J, as a simple object in $\mathcal{Z}(\mathscr{F})$, may carry multiple types of internal degree of freedom p, thereby enlarging its internal gauge space. Although these p are gauge degrees of freedom and hence unobservable in the topological phase, they play a central role in the construction of the CFT states, where topological invariance is broken to expose these internal degrees of freedom, which become physical local degrees of freedom determine the physical phenomena that may be captured by a critical CFT.

In the HGW model, anyons are created in pairs by acting a *creation operator* on the ground state $|\Psi\rangle$. It suffices to define the action of the shortest creation operator $W_E^{J;pq}$, which creates a pair of dyons (J^*, p^*) and (J, q) in the two adjacent plaquettes separated by an edge E:

$$W_E^{J;pq}$$ 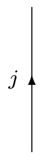 $$:= \sum_{k \in L_{\mathscr{F}}} \sqrt{\frac{d_k}{d_j}}\, \overline{z_{pqj}^{J;k}}$$ 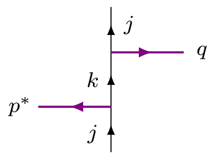 , (1.1)

where J is a simple object in $\mathcal{Z}(\mathscr{F})$, p, q are internal gauge degrees of freedom on tails of anyons, j is the degree of freedom on edge E, and $z_{pqj}^{J;k}$ is the coefficients called *half-braiding tensors*. All other creation operators in the model can be generated by composing such shortest creation operators. .

In a companion paper[3], it is shown that the edges of the lattice carry a flat gauge field valued in $\mathscr{F}$, and the open ends of the tails host anyon excitations coupled with the gauge field via the Gauss law and gauge connection. This finding allows one to recast topological phases back in the Landau-Ginzburg paradigm, though in a more general sense, where phase transitions are triggered by anyon condensation. The HGW model is a convenient framework for constructing any possible kind of anyon condensation in a doubled topological phase and study the consequent phenomena[3].

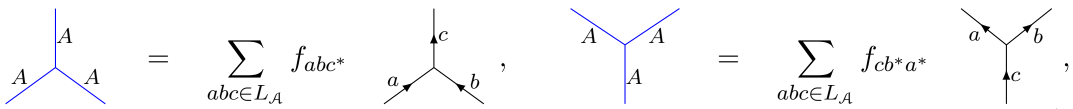

(1.2)

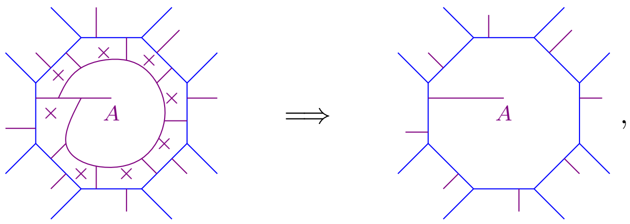

1.1 Definitions of Frobenius Algebras and Modules

In this appendix, we quickly review the mathematical definitions of Frobenius algebras and modules. One who wants to construct their own CFTs via our method can take use of the definition of Frobenius algebras and modules in this section.

A unitary Frobenius algebra in $\mathscr{F}$ is a (possibly composite) objects in $\mathscr{F}$ i.e.

$$\mathcal{A} = \bigoplus_a n_a a, \qquad a \in \mathscr{F}, \qquad n_a \in \mathbb{N}, \tag{1.3}$$

equipped with a product $\mathcal{A} \otimes \mathcal{A} \to \mathcal{A}$ and coproduct $\mathcal{A} \to \mathcal{A} \otimes \mathcal{A}$, satisfying certain properties. Here, n_a are non-negative integers describing the multiplicities of object $a \in \mathscr{F}$ participating in $\mathcal{A}$. To avoid clutter, the discussion in this section is limited to $n_a \leq 1$, although it can be readily generalized by introducing extra indices i for each anyon label $a \in \mathcal{A}$ whose $n_a > 1$. For the case where all $n_a \leq 1$, the products and co-products of $\mathcal{A}$ encoded in a cyclically symmetric function $f^{\mathcal{A}} : L_{\mathcal{A}}^3 \to \mathbb{C}$, satisfying

$$\sum_{t\in L_{\mathcal{A}}} f^{\mathcal{A}}_{rst} f^{\mathcal{A}}_{abt^*} G^{rst}_{abc} \sqrt{d_c d_t} = f^{\mathcal{A}}_{acs} f^{\mathcal{A}}_{rc^*b} \ , \tag{1.4}$$

$$\sum_{ab\in L_{\mathcal{A}}} f^{\mathcal{A}}_{abc} f^{\mathcal{A}}_{c^*b^*a^*} \sqrt{d_a d_b} = d_{\mathcal{A}} \sqrt{d_c}, \tag{1.5}$$

$$f^{\mathcal{A}}_{abc} = f^{\mathcal{A}}_{bca}, \quad f^{\mathcal{A}}_{1ab} = \delta_{ab^*}, \quad f^{\mathcal{A}}_{abc} = (f^{\mathcal{A}}_{c^*b^*a^*})^*. \tag{1.6}$$

where $L_{\mathcal{A}} = \{a \in \mathscr{F} : n_a = 1\}$ is the set of simple objects appearing in $\mathcal{A}$, and $d_{\mathcal{A}} = \sum_{a\in L_{\mathcal{A}}} d_a$ is the quantum dimension of $\mathcal{A}$. One can express this map in basis form, which is depicted in figure 1.

A right module of Frobenius algebra $\mathcal{A}$ in a UFC $\mathscr{F}$ is a (possibly composite) object

$$M_{\mathcal{A}} := \bigoplus_{x\in L_{\mathscr{F}}} m_x x,$$

equipped with an algebra action on $M_{\mathcal{A}}$: $M_{\mathcal{A}} \otimes \mathcal{A} \to M_{\mathcal{A}}$. Here, x is a collection of simple objects of $\mathscr{F}$ that appear in the module, and $m_x \in \mathbb{N}$ is the multiplicity of x in M. For

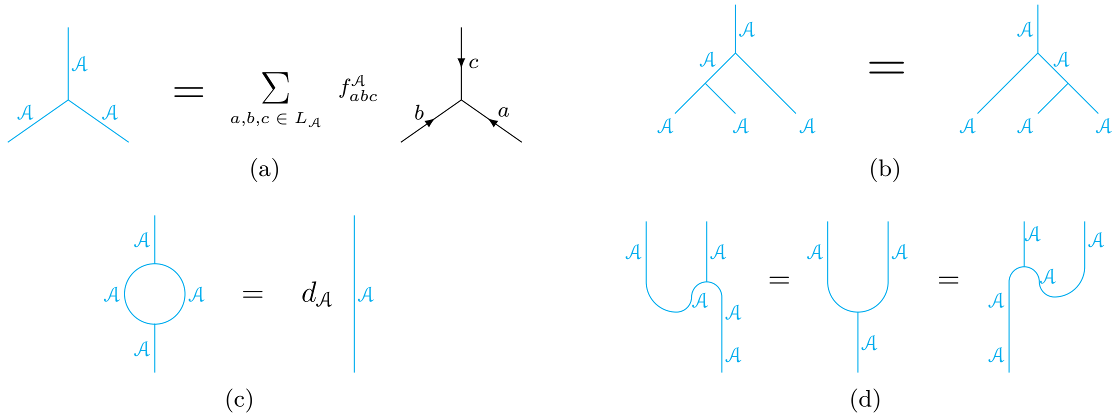

Figure 1: (a) Frobenius algebras in basis form. (b) The Associativity: Eq. (1.4). (c) The unitarity: Eq. (1.5). (d) Equations (1.6). Taking different graphical bases yields different equations in Eq. (1.6). This equation is equivalent to the Frobenius condition[4].

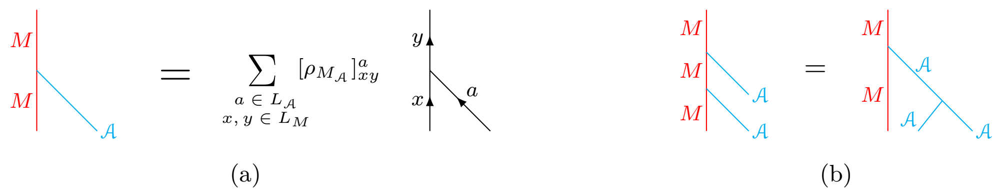

Figure 2: (a) The basis representation of right-A module M. (b) The right-module condition: Eq. (1.7).

simplicity, in this paper, we restrict to the case $m_x \leq 1$, and define $L_{M_{\mathcal{A}}} = \{x \in L_{\mathscr{F}} \mid m_x = 1\}$. The algebra action is recorded in a *module function* $\rho_{M_{\mathcal{A}}} : L_{\mathcal{A}} \otimes L^2_{M_{\mathcal{A}}} \to \mathbb{C}$, which satisfies an associativity constraint:

$$[\rho_{M_{\mathcal{A}}}]^a_{xy} [\rho_{M_{\mathcal{A}}}]^b_{yz} G^{bz^*by}_{xac} = f^{\mathcal{A}}_{abc^*} [\rho_{M_{\mathcal{A}}}]^c_{xz}, \qquad [\rho_{M_{\mathcal{A}}}]^a_{xy} = ([\rho_{M_{\mathcal{A}}}]^{a^*}_{x^*y^*})^*. \tag{1.7}$$

In particular, for UFC $\mathtt{Vec}(G)$ with a finite group G, the modules over a Frobenius algebra $\mathcal{A} = \bigoplus_{g\in H} g$ (with multiplication $f^{\mathcal{A}}_{fgh} = \delta_{e,fgh}$) for a subgroup $H \leq G$ correspond to the representations of H, and function ρ encode the representation matrix entries.

One can express the module function in basis form, which is depicted in figure 2: The vertex connecting the edges colored by $\mathcal{A}$ and the chosen module $M_{\mathcal{A}}$ are weighted by the coefficients $[\rho_{M_{\mathcal{A}}}]^a_{xy}$ that defines the action of $\mathcal{A}$ on the module.

1.2 Anyon Condensation in the HGW Model

The HGW model provides a finer description of anyon-condensation-induced topological phase transitions.

To describe the procedure of condensing a Lagrangian set L of anyons in the HGW

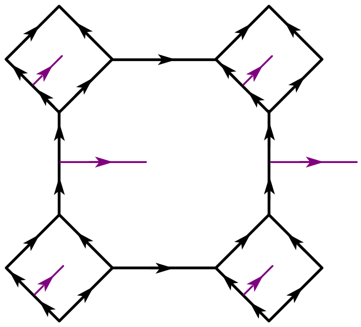

Figure 3: The HGW model.

model, we can add to the HGW Hamiltonian a condensation term:

$$H = H_{\mathscr{F}} - \lim_{\Lambda\to\infty} \sum_{E} P_E^{\mathcal{A}},$$

where $H_{\mathscr{F}}$ is HGW Hamiltonian of the parent topological phase, and $P_E^{\mathcal{A}}$ is a local projector acting on an edge E:

$$P_E^{\mathcal{A}} = \sum_{J\in L} \quad \sum_{p,q} \pi_J^{p,q} W_E^{J;pq} \; = {}_E|\mathcal{A}\rangle\langle\mathcal{A}|_E,$$

where $W_E^{J;pq}$ are creation operators of condensed dyons, $\pi_J^{p,q} \in \mathbb{C}$ are coefficients to make the sum a projector. In the limit $\Lambda \to \infty$, projectors $P_E^{\mathcal{A}}$ ensures that the new ground states $|\mathcal{A}\rangle_E$ are $+1$ eigenstates of all $P_E^{\mathcal{A}}$, which are coherent states filled with arbitrarily many condensed anyons throughout the lattice. This state can be locally represented as:

$|A\rangle_E =$ 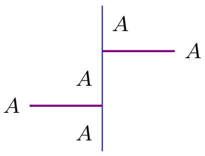

$= \sum_{j,k,p,q\in L_{\mathcal{A}}} f_{jk^*p^*} f_{kq^*j^*}$ 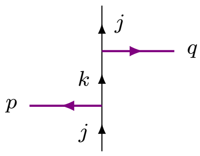

,

where E is an edge of the lattice, while the violet lines refer to auxiliary tails in plaquettes, which will then be contracted via topological moves and result in only one tail in each plaquette, representing the entanglements between different edges. The global ground state of the trivial topological order is the state where each edge and tail in the square-octagon lattice carries Frobenius algebra object A.

In the case of the Doubled Ising model, there are two Frobenius algebras of the input Ising UFC:

$$\mathcal{A}_1 = 1, \qquad [f_1]_{111} = 1, \qquad \mathcal{A}_2 = 1 \oplus \psi, \qquad [f_2]_{111} = [f_2]_{1\psi\psi} = 1.$$

These two input Frobenius algebras are Morita equivalent because they have the same full center $L = 1\bar{1} \oplus \psi\bar{\psi} \oplus \sigma\bar{\sigma}$. The corresponding projectors are

$$P_E^{\mathcal{A}_1} = \frac{W_E^{1\bar{1};1,1} + W_E^{\psi\bar{\psi};1,1} + 2W_E^{\sigma\bar{\sigma},1,1}}{4} = \delta_{j_E,0}, \qquad P_E^{\mathcal{A}_2} = \frac{W_E^{1\bar{1};1,1} + W_E^{\psi\bar{\psi};1,1} + 2W_E^{\sigma\bar{\sigma},\psi,\psi}}{4}. \tag{1.8}$$

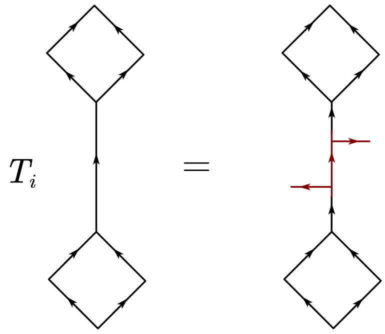

Figure 4: Anyon creation operator

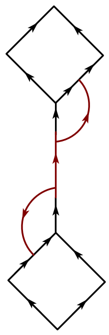

Figure 5: Anyon condensation

82 In our square-octagon lattice as shown in the main text, the anyon operator, the pair creation operator should act as shown in figure 4. The HGW lattice is different from the HGW string net with these extra tails. To make contact with the original version of the strange correlator which follows from the HGW ground state wave-function, we would like to remove these tails. One very natural way of achieving this is to connect these lines to the square, as shown in figure 5, and then removing the extra bubble by F-moves.

We note that the Ising critical state

$$\langle \;{}_{\text{critical}}| = \frac{1}{2}\left((\sqrt{2}+1)\langle \;{}^{1}_{\sigma}\,| + \langle \;{}^{\psi}_{\sigma}\,|\right), \tag{1.9}$$

is the eigenstate of $P_E^{\mathcal{A}_1} + P_E^{\mathcal{A}_2}$ with the largest eigenvalue.

This story can be repeated in all pair-competition in which $\mathcal{A}_i \subset \mathcal{A}_j$ in other fusion category. The predicted phase transition between pair-competition is

$$\langle \;{}_{(\mathcal{A}_i, M_{\mathcal{A}_i}),(\mathcal{A}_j, M_{\mathcal{A}_j})}|_{\text{critical}} = \langle \widehat{\mathcal{A}}_i|_{M_{\mathcal{A}_i}} + \langle \widehat{\mathcal{A}}_j|_{M_{\mathcal{A}_j}} \tag{1.10}$$

One can show that this is always the eigenstate with the largest eigenvalue of the sum of projection operators, analogously defined as the Ising case above, irrespective of the choice of the common module between $\mathcal{A}_{i,j}$.

1.3 Lagrangian Algebra of Anyon Condensation

Now, after anyon condensation via a specific projector $P_E^{\mathcal{A}}$, the resulting model is a trivial topological phase with a one-dimensional Hilbert space spanned by $|\mathcal{A}\rangle_E$. The projector $P_E^{\mathcal{A}}$ is defined as

$$P_E^{\mathcal{A}} = |\mathcal{A}\rangle_{EE}\langle\mathcal{A}| = \sum_{J\in L}\sum_{p,q} \pi_J^{p,q}\, W_E^{J;pq}.$$

Solving this equation, the coefficients $\pi_J^{p,q}$ encapsulate all information about the Lagrangian algebra L associated with the anyon condensation.

More explicitly, those anyon types J with $\pi_J^{pq} \neq 0$ are precisely the condensed anyons appearing in the Lagrangian algebra. It can be proven[3] that all condensed anyons are bosonic and braid trivially with each other.

There may exist multiple dyonic sectors of the same anyon type J that condense simultaneously; these are called the condensed sectors of J. The number n_{Cond}^J of condensed sectors for anyon J is referred to as the *multiplicity* of condensed anyon J during anyon condensation. Collect the condensation coefficients π_J^{pq} for a fixed anyon type J into a matrix:

$$\Pi^J = \begin{pmatrix} \pi_J^{p_1p_1} & \pi_J^{p_1p_2} & \cdots \\ \pi_J^{p_2p_1} & \pi_J^{p_2p_2} & \cdots \\ \vdots & \vdots & \ddots \\ \pi_J^{p_{n_J^p}p_1} & \pi_J^{p_{n_J^p}p_2} & \cdots \end{pmatrix}.$$

Then,

$$n_{\text{Cond}}^J = \text{rank}(\Pi^J).$$

The corresponding Lagrangian algebra of the modular tensor category $\mathcal{Z}(\mathcal{F})$ is thus

$$L = \bigoplus_{J\in L_{\text{Cond}}} n_{\text{Cond}}^J\, J.$$

We can further diagonalize the condensation matrix using a unitary transformation U_J:

$$U_J \Pi^J U_J^\dagger = \text{diag}\{\pi_J^1, \pi_J^2, \ldots, \pi_J^{n_{\text{Cond}}^J}, 0, 0, \ldots, 0\},$$

where $\pi_J^i \in \mathbb{C}$ and $1 \leq i \leq n_{\text{Cond}}^J$. The i-th condensed sector of anyon J is then given by

$$|J, i\rangle_{\text{Cond}} = \sum_p \frac{1}{d_p}\, [U_J]_{ip} |J, p\rangle,$$

and its corresponding creation operator is

$$\tilde{W}_E^{J_i} = \sum_{p,q} \frac{1}{d_p d_q}\, [U_J^\dagger]_{J_i p}\, W_E^{J;pq}\, [U_J]_{qJ_i}, \tag{1.11}$$

where the sums run over the T-charges of anyon J. The condensation projector $P_E^{\mathcal{A}}$ can now be written as a sum of these normalized creation operators:

$$P_E^{\mathcal{A}} = \frac{1}{d_{\mathcal{A}}} \sum_{\text{Condensed } J} \sum_{i=1}^{n_{\text{Cond}}^J} \tilde{W}_E^{J_i},$$

which faithfully realize the algebra basis elements of the Lagrangian algebra L. In particular, the operator product expansion coefficients of these creation operators encode the algebra multiplication structure of L:

$$W_E^{J_i} W_E^{K_j} = \sum_{M_k} f_{J_i K_j}^{M_k} W_E^{M_k}.$$

2 Some Details of Various Categories

2.1 The Modular Tensor Category $\mathcal{Z}(S_3)$

We would like to review here some basic data of the $\mathcal{Z}(S_3)$ category. The symmetry group $S_3 = \langle x, y | x^3 = y^2 = e, yx = x^2 y\rangle$. The anyons of $\mathcal{Z}(S_3)$ are labeled by a pair (W, γ_W), where W is a conjugacy class of the group S_3, and γ_W an irreducible representation of the centralizer of W. There're eight kinds of anyons in $\mathcal{Z}(S_3)$, conventionally labelled by letters A through H. A summary of all the anyons are listed below.

	A	B	C	D	E	F	G	H
conjugacy class W	$\{e\}$			$\{y, xy, x^2y\}$		$\{x, x^2\}$		
centralizer $\cong$	S_3			$\mathbb{Z}_2$		$\mathbb{Z}_3$		
irrep γ_W of centralizer	$\mathbf{1}$	sign	π	$\mathbf{1}$	$-\mathbf{1}$	$\mathbf{1}$	ω	ω^*
$\dim(\gamma_W)$	1	1	2	1	1	1	1	1
quantum dimension $d = \|W\| \times \dim(\gamma_W)$	1	1	2	3	3	2	2	2
twist θ	1	1	1	1	-1	1	$e^{2\pi i/3}$	$e^{-2\pi i/3}$

Their fusion rules are given by

$\otimes$	A	B	C	D	E	F	G	H
A	A	B	C	D	E	F	G	H
B	B	A	C	E	D	F	G	H
C	C	C	$A\oplus B\oplus C$	$D\oplus E$	$D\oplus E$	$G\oplus H$	$F\oplus H$	$F\oplus G$
D	D	E	$D\oplus E$	$A\oplus C\oplus F\oplus G\oplus H$	$B\oplus C\oplus F\oplus G\oplus H$	$D\oplus E$	$D\oplus E$	$D\oplus E$
E	E	D	$D\oplus E$	$B\oplus C\oplus F\oplus G\oplus H$	$A\oplus C\oplus F\oplus G\oplus H$	$D\oplus E$	$D\oplus E$	$D\oplus E$
F	F	F	$G\oplus H$	$D\oplus E$	$D\oplus E$	$A\oplus B\oplus F$	$C\oplus H$	$C\oplus G$
G	G	G	$F\oplus H$	$D\oplus E$	$D\oplus E$	$C\oplus H$	$A\oplus B\oplus G$	$C\oplus F$
H	H	H	$F\oplus G$	$D\oplus E$	$D\oplus E$	$C\oplus G$	$C\oplus F$	$A\oplus B\oplus H$

There're 4 distinct Lagrangian algebras in $\mathcal{Z}(S_3)$, labeled by the 4 different subgroups of S_3. The Lagrangian algebras corresponding to each subgroup are listed in the following table.

subgroup K	Lagrangian algebra L
$\mathbb{1}$	$A \oplus B \oplus 2C$
$\mathbb{Z}_2$	$A \oplus C \oplus D$
$\mathbb{Z}_3$	$A \oplus B \oplus 2F$
S_3	$A \oplus D \oplus F$

2.2 Haagerup Fusion Category H_3

The *Haagerup* fusion category is a notably special category. It contains six types of simple objects, labeled by

$$1, \qquad \alpha, \qquad \alpha^2, \qquad \rho, \qquad \alpha\rho, \qquad \alpha^2\rho,$$

with the following quantum dimensions

$$d_1 = d_\alpha = d_{\alpha^2} = 1, \qquad d_\rho = d_{\alpha\rho} = d_{\alpha^2\rho} = \frac{3+\sqrt{13}}{2}.$$

The fusion rules are

1	α	α^2	ρ	$\alpha\rho$	$\alpha^2\rho$
α	α^2	1	$\alpha\rho$	$\alpha^2\rho$	ρ
α^2	1	α	$\alpha^2\rho$	ρ	$\alpha\rho$
ρ	$\alpha^2\rho$	$\alpha\rho$	$1 \oplus \rho \oplus \alpha\rho \oplus \alpha^2\rho$	$\alpha^2 \oplus \rho \oplus \alpha\rho \oplus \alpha^2\rho$	$\alpha \oplus \rho \oplus \alpha\rho \oplus \alpha^2\rho$
$\alpha\rho$	ρ	$\alpha^2\rho$	$\alpha \oplus \rho \oplus \alpha\rho \oplus \alpha^2\rho$	$1 \oplus \rho \oplus \alpha\rho \oplus \alpha^2\rho$	$\alpha^2 \oplus \rho \oplus \alpha\rho \oplus \alpha^2\rho$
$\alpha^2\rho$	$\alpha\rho$	ρ	$\alpha^2 \oplus \rho \oplus \alpha\rho \oplus \alpha^2\rho$	$\alpha \oplus \rho \oplus \alpha\rho \oplus \alpha^2\rho$	$1 \oplus \rho \oplus \alpha\rho \oplus \alpha^2\rho$

2.2.1 Frobenius Algebras and Modules

The Haagerup category has seven Frobenius algebras divided into three Morita classes. The Haagerup fusion rules are not commutative, so the left and right modules are slightly different. We only consider the right modules here. The module function tensor component $[\rho^{\mathcal{A}}_M]^a_{xy}$ represents the algebra object $a \in \mathcal{A}$ fuses from right to module object $x \in M$ and transform it to $y \in M$, i.e., $y \in x \otimes a$. The three minimal algebras along with their modules are listed below:

1. The trivial Frobenius algebra $\mathcal{A}_0 = \mathbf{1}$, such that $f^{\mathbf{11}}_{\mathbf{1}} = 1$. It has six *right* modules: $M_x = x, \rho^{\mathbf{1}}_{xx} = \mathbf{1}$, where x is a Haagerup simple object.

2. The $\mathbb{Z}_3$ Frobenius algebra $\mathcal{A}_2 = \mathbf{1} \oplus \alpha \oplus \alpha^2$, such that $f^{bc}_a = N^{bc}_a$, the fusion rules. It has two simple modules:

$$M_{\mathbf{1}} = \mathbf{1} \oplus \alpha \oplus \alpha^2, \qquad [\rho_{\mathbf{1}}]^a_{xy} = N^{xa}_y,$$

$$M_\rho = \rho \oplus \alpha\rho \oplus \alpha^2\rho, \qquad [\rho_\rho]^a_{xy} = N^{xa}_y (-1)^{\delta_{a,\alpha^2}\delta_{x,\alpha\rho}\delta_{y,\alpha^2\rho}},$$

3. The special Frobenius algebra $\mathcal{A}_4 = \mathbf{1} \oplus \rho \oplus \alpha\rho$. The algebra multiplication f_a^{bc} is too cumbersome to write here. It has four simple right modules:

$$M_{\mathbf{1}} = \mathbf{1} \oplus \rho \oplus \alpha\rho, \qquad [\rho_{\mathbf{1}}]_{xy}^a = f_y^{xa}.$$

$$M_\alpha = \alpha \otimes M_{\mathbf{1}} = \alpha \oplus \alpha\rho \oplus \alpha^2\rho, \qquad [\rho_\alpha]_{xy}^a = \frac{f_y^{xa}}{[F_y^{\alpha,\alpha^2\otimes x,a}]_{x,\alpha^2\otimes y}}.$$

$$M_{\alpha^2} = \alpha^2 \otimes M_{\mathbf{1}} = \alpha^2 \oplus \rho \oplus \alpha^2\rho, \qquad [\rho_{\alpha^2}]_{xy}^a = \frac{f_y^{xa}}{[F_y^{\alpha^2,\alpha\otimes x,a}]_{x,\alpha\otimes y}},$$

$$M_\rho = \rho \oplus \alpha^2\rho \oplus \alpha\rho.$$

The module function of M_ρ is somewhat messy and will not be presented in the text.

The other connected Frobenius algebras can be obtained by conjugating these minimal algebras with some simple objects. The modules of the other non-minimal Frobenius algebras can be easily calculated from those of the minimal ones. We take $\mathcal{A}_5 = \alpha \otimes \mathcal{A}_4\alpha^2$ as an illustrating example. For M_i any right-$\mathcal{A}_4$ module, $M_i \otimes \alpha^2$ must be a right-$\mathcal{A}_5$ module. And the module function of $M_i \otimes \alpha^2$ (on $\mathcal{A}_5$) differ from M_i (on $\mathcal{A}_4$) only by some F-symbols, which can be determined immediately. We summarize all the algebras, their right-modules and the refined condensation tree below.

$\mathcal{A}$	Right-$\mathcal{A}$ modules
$\mathbf{1}$	Every simple object is an independent module
$\rho \otimes \rho$	$i \otimes \rho$ where i is any simple object
$\mathbf{1} \oplus \alpha \oplus \alpha^2$	$\mathbf{1} \oplus \alpha \oplus \alpha^2$, $\rho \otimes (\mathbf{1} \oplus \alpha \oplus \alpha^2)$
$\rho \otimes (\mathbf{1} \oplus \alpha \oplus \alpha^2) \otimes \rho$	$(\mathbf{1} \oplus \alpha \oplus \alpha^2) \otimes \rho$, $\rho \otimes (\mathbf{1} \oplus \alpha \oplus \alpha^2) \otimes \rho$
$\mathbf{1} \oplus \rho \oplus \alpha\rho$	$\mathbf{1} \oplus \rho \oplus \alpha\rho$, $\alpha \otimes (\mathbf{1} \oplus \rho \oplus \alpha\rho)$, $\alpha^2 \otimes (\mathbf{1} \oplus \rho \oplus \alpha\rho)$, $\rho \oplus \alpha\rho \oplus \alpha^2\rho$
$\alpha \otimes (\mathbf{1} \oplus \rho \oplus \alpha\rho) \otimes \alpha^2$	$M \otimes \alpha^2$ where M is any right module of $\mathbf{1} \oplus \rho \oplus \alpha\rho$
$\alpha^2 \otimes (\mathbf{1} \oplus \rho \oplus \alpha\rho) \otimes \alpha$	$M \otimes \alpha$ where M is any right module of $\mathbf{1} \oplus \rho \oplus \alpha\rho$

3 Critical Strange Correlator of the Ising Category

As an example, we explicitly write down the local transfer matrix for competing Ising anyons. The predicted critical unit cell (1.9) reads

$$M_{\sigma\sigma\sigma\sigma 1} = (\sqrt{2}+1)/2, M_{\sigma\sigma\sigma\sigma\psi} = 1/2,$$

which give rise to the local transfer matrix for a unit cell

$$z_{b_1b_2b_3b_4e,i_1i_2k_1k_2} = \sqrt[4]{d_e^2 d_{b_1} d_{b_2} d_{b_3} d_{b_4} d_{i_1} d_{i_2} d_{k_1} d_{k_2}} M_{b_1b_2b_3b_4e} \begin{bmatrix} b_1 & e & b_2 \\ i_2 & k_1 & i_1 \end{bmatrix} \begin{bmatrix} b_3 & e & b_4 \\ i_2 & k_2 & i_1 \end{bmatrix} \tag{3.1}$$

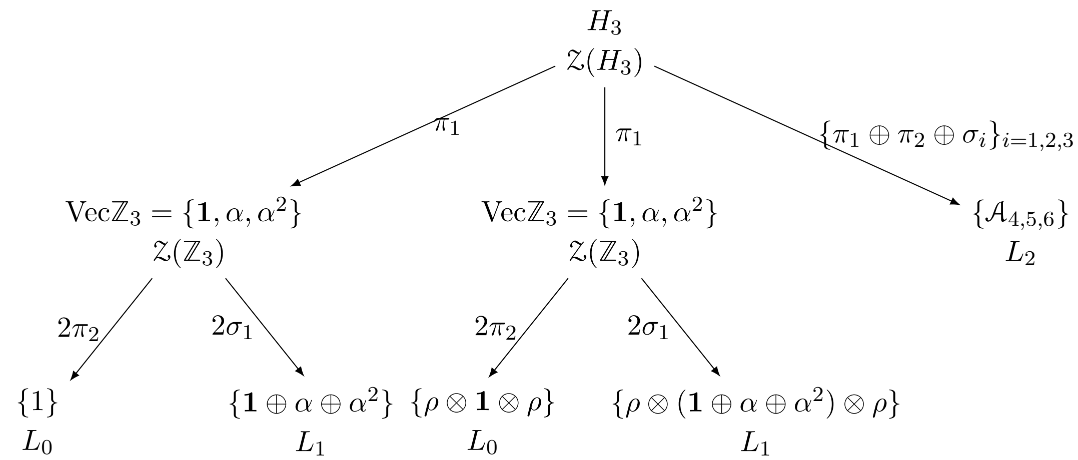

Figure 6: Condensation tree for the doubled H_3 symTO. The right most branch abbreviates the 3 Morita equivalent branches, with the Frobenius algebras involved given above.

We omit $b_1 = b_2 = b_3 = b_4 = \sigma$ and sum over the inner index e to

$$z_{\sigma\sigma 11} = \sqrt{2}+1, z_{\sigma\sigma\psi\psi} = \sqrt{2}+1, z_{\sigma\sigma 1\psi} = 1, z_{\sigma\sigma\psi 1} = 1, \tag{3.2a}$$

$$z_{11\sigma\sigma} = \sqrt{2}+1, z_{\psi\psi\sigma\sigma} = \sqrt{2}+1, z_{1\psi\sigma\sigma} = 1, z_{\psi 1\sigma\sigma} = 1. \tag{3.2b}$$

If we interpret 1 and ψ as spin up and down, each line in (3.2) gives one independent copy of the local weights $e^{2\beta} = \sqrt{2}+1$ for a classical Ising model with the critical inverse temperature $\beta = \frac{1}{2}\ln(\sqrt{2}+1)$. The object σ acts as a placeholder to keep these two copies disentangled.

We thus conclude that the strange correlator with the critical unit cell (1.9) is a partition function of two copies of critical Ising.

4 The Effect of the Collection of Objects $M_{\mathcal{A}_i} \neq M_{\mathcal{A}_j}$ in the interpolation in a unit cell

We emphasized in the main text that to deconstruct the competition of condensates in the global lattice into competitions within the unit cells, it is crucial to color the slanted edges in the unit cell by module $M_{\mathcal{A}_{i,j}}$ such that these modules contain exactly the same set of objects, even though generically module functions could differ.

Here, we illustrate with examples that when $M_{\mathcal{A}_i}$ and $M_{\mathcal{A}_j}$ contain different objects, condensates in neighbouring unit cells would be entangled non-trivially. The equilibrium constructed within one unit cell in (1.10) would be disrupted by its neighbors.

As an illustration, let us consider the Ising model. We again consider the competition between $\mathcal{A}_1 = \mathbf{1}$ and $\mathcal{A}_2 = \mathbf{1} \oplus \psi$ with however the following interpolation

$$\langle \succ\!\!\prec_{(\mathcal{A}_1,\sigma),(\mathcal{A}_2,1\oplus\psi)} | = \langle \widehat{\mathcal{A}}_1|_\sigma + r\langle \widehat{\mathcal{A}}_2|_{1\oplus\psi}, \tag{4.1}$$

where we have chosen $M_{\mathcal{A}_1} = \sigma$ and $M_{\mathcal{A}_2} = \mathbf{1} \oplus \psi$. Now consider assembling the global $|\Omega\rangle$ from this unit cell, as indicated in the Figure 1 of the main text. It is clear that for two

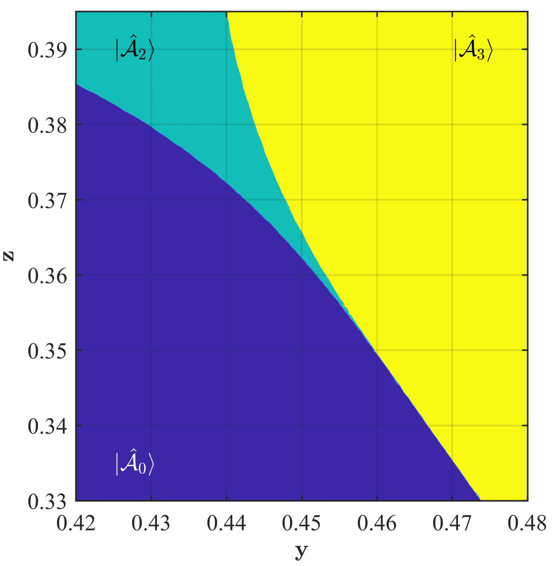

Figure 7: Close-up view of the $\mathcal{A}_5$ phase diagram near the tri-critical point, colored according to the converged tensor.

neighbouring unit cells connected by a slanted edge in which the module runs, when $\mathcal{A}_1$ appears in one unit cell, all of its neighbours must also be $\mathcal{A}_1$, and as a result all unit cells are forced into $\mathcal{A}_1$. Similarly when $\mathcal{A}_2$ appears in one unit cell, all unit cells in the global state are simultaneousely $\mathcal{A}_2$. Each of these corresponds to a global RG fixed point state of a globally condensed phase.

There is thus complete correlation between all unit cells, and the equilibrium intended for a single unit cell in equation (1.10) did not correspond to the phase transition point as r is varied. Instead, it is found that the critical coupling occurs at $r_c = 2^{1/4} = \sqrt{\frac{d_{M_{\mathcal{A}_2}}}{d_{M_{\mathcal{A}_1}}}}$. One can readily check that this is equivalent to the equal weight summation of the $\mathcal{A}_1$ and $\mathcal{A}_2$ condensate, with normalisation defined by the *global lattice* instead of the unit cell. Also, given that the entire global lattice now plays the role of the unit cell, the dimension of phase space is huge and not surprisingly the phase transition point is first order.

When the module objects are common between $M_{\mathcal{A}_i}$ and $M_{\mathcal{A}_j}$, one can readily show that every module object in one unit cell to be fed to the next neighbouring cell would be acted upon by every member of the condensate in the linear combination of condensates in the next cell. Therefore each unit cell forms a common background to all the condensates appearing in its neighbour cell. As a result equilibrium achieved in a unit cell is not disrupted by its neighbour. The unit cells are essentially factorised as desired.

5 Locating the tri-critical point in the $\mathcal{A}_5$ phase diagram

In the $\mathcal{A}_5$ phase diagram, there appears to be a discrepancy between the analytically predicted and numerically observed locations of the tri-critical point. We now resolve this

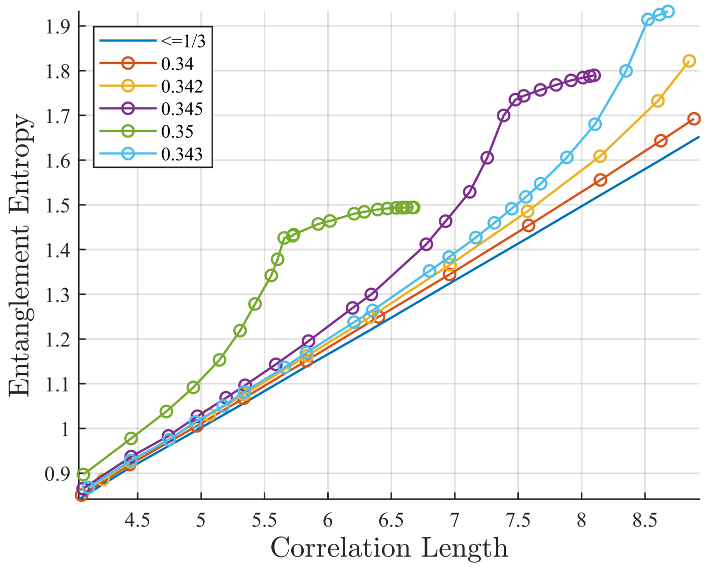

Figure 8: Entanglement scaling for different values of z along the KW dual line of the $\mathcal{A}_5$ phase diagram.

issue.

Analytically, the partition function along the KW duality line can be mapped to the duality line of the well-known Ashkin–Teller (AT) model. The $c = 1$ critical segment of the AT model corresponds to the KW dual line in our model for $0 \le z \le \frac{1}{3}$, with $z = \frac{1}{3}$ marking the tri-critical point [5]. Beyond this point, the critical line bifurcates into two distinct Ising-critical branches.

A magnified phase diagram is shown in Figure 7. The separation of the two Ising critical lines becomes visible around $z \approx 0.35$, below which they appear to merge into a single critical line. For $z \le 0.35$, we switch to the entanglement scaling method [6], which, although computationally too expensive to map the entire diagram, provides more reliable identification of critical points than our TNR algorithm at hand.

In Figure 8, we plot the entanglement entropy versus correlation length along the KW duality line $z = -\sqrt{2}y + 1$. For $z \le \frac{1}{3}$, all data fall on the same $c = 1$ line. For larger z, however, the plots exhibit varying slopes. At small bond dimension (the lower part of each plot, corresponding to less coarse-grained system sizes), the data initially suggest a CFT with effective central charge $c > 1$. As the bond dimension increases, the scaling crosses over to a line with central charge $c \approx 0.5$ before eventually saturating, indicating a gapped phase. Slightly above $z = \frac{1}{3}$, such as at $z = 0.342$, the data form an almost straight line with apparent $c > 1$. We believe for sufficiently large bond dimensions a crossover to the $c = 0.5$ line would appear, followed by saturation. Nevertheless, these observations indicate that parts of the seemingly $c \approx 1$ region actually arise from two closely spaced Ising CFT lines. In our parametrization, VUMPS calculations confirm that the distance between the two branches is approximately 3×10^{-5} at $z = 0.35$, consistent with the barely discernible separation observed in the phase diagram (Fig. 7).

References

[1] Y. Hu, N. Geer, and Y.-S. Wu, "Full dyon excitation spectrum in extended levin-wen models," *Physical Review B* **97** no. 19, (2018) 195154.

[2] Y. Zhao and Y. Wan, "Noninvertible gauge symmetry in (2+ 1) d topological orders: A string-net model realization," *arXiv preprint arXiv:2408.02664* (2024) .

[3] Y. Zhao and Y. Wan, "Nonabelian anyon condensation in 2+1d topological orders: A string-net model realization," *JHEP* **05** (2025) 156, `arXiv:2409.05852 [cond-mat.str-el]`.

[4] Y. Hu, Z.-X. Luo, R. Pankovich, Y. Wan, and Y.-S. Wu, "Boundary hamiltonian theory for gapped topological phases on an open surface," *Journal of High Energy Physics* **2018** no. 1, (2018) 1–41.

[5] Y. Aoun, M. Dober, and A. Glazman, "Phase Diagram of the Ashkin–Teller Model," *Commun. Math. Phys.* **405** no. 2, (2024) 37.

[6] L. Vanderstraeten, J. Haegeman, and F. Verstraete, "Tangent-space methods for uniform matrix product states," *SciPost Phys. Lect. Notes* **7** (2019) 1, `arXiv:1810.07006`.